Submitted to IGS Remote Sensing Symposium, June 2001

Surface Elevation Changes in West Antarctica from Satellite Radar Altimetry: Mass Balance Implications

H. Jay Zwally[1], Anita C. Brenner[2], and Helen Cornejo[2]

1. Ocean and Ice Branch Code 971, NASA/Goddard Space Flight center, Greenbelt, MD 20771, USA

2. Raytheon ITSS Code 971, NASA/Goddard Space Flight center, Greenbelt, MD 20771, USA

Abstract

Time-series of surface elevation change, which are constructed from 7-years (1992-1999) of ERS-1 and 2 satellite radar altimeter data of Antarctica, show significant seasonal, inter-annual, and long-term changes. Elevation time-series are created from altimeter crossovers among 90-day data periods on a 50 km grid to 81.5° S and fit with a multivariate linear/sinusoidal function to give the average rate of elevation change (dH/dt) and account for seasonal changes. On the major Ronne, Filchner, and Ronne ice shelves, the dH/dt are small or near zero. In contrast, the ice shelves of the Antarctic Peninsula and along the West Antarctic coast appear to be thinning significantly, with a 23 ± 3 cm a^{-1} surface elevation decrease on the Larsen ice shelf and a 65 ± 4 cm a^{-1} decrease on the Dotson ice shelf. Significant elevation decreases are obtained over most of the drainage basins of the Pine Island and Thwaites glaciers. Significant increases are obtained over most of the other grounded ice in Marie Byrd Land, the Antarctic Peninsula, and Coates Land. Over the sector from 85° W to 115° W, which includes the Pine Island and Thwaites basins, the average elevation is significantly decreasing by 8.1 cm a^{-1}. The corresponding ice thickness change is about -11 cm a^{-1}, with a corresponding mass loss of 82 Gt a^{-1}, and a 0.22 mm a^{-1} contribution to global sea level rise. In terms of elevation change, the decrease in the Pine Island-Thwaites sector sector is largely balanced by the increase in the Marie Byrd Land, but only balanced by about 1/4 in terms of ice thickness change and contribution to sea level rise. The overall average elevation change for the grounded ice is + 1.2 cm a^{-1}. Using an average bedrock uplift of 2.5 cm a^{-1} , implies an average ice thickness decrease of 1.3 cm a^{-1}, a mass loss of 22 Gt a^{-1}, and a 0.06 mm a^{-1} contribution to global sea level rise.

INTRODUCTION

The state of mass balance and dynamic stability of the West Antarctic ice sheet has been the subject of considerable research and discussion in recent decades (e.g. Bentley, 1997; Bindschadler, 1998; Oppenheimer, 1998). Highlights of the research program include the discovery that ice streams draining into the Ross Ice shelf have either increased their rates of discharge, slowed down, or even ceased to flow as ice streams (Alley and Bindschadler, 2001). Recently, attention has focused on the Pine Island glacier flowing into the Amundsen Sea and its drainage system (Vaughan and others, 2000). For example, recent analysis of SAR interferometry showed the position of the hinge line of the Pine Island glacier retreated 1.2 km a^{-1} between1992 and 1996 (Rignot, 1998). Shepherd and others (2001), using data from ERS-1 and 2 radar altimetry for 1992 to 1999, found an elevation decrease of 75 ± 7 cm a^{-1} on the Pine Island glacier trunk, and a mean thinning of 11 ± 1 cm a^{-1} extending inland over the basin. Previously, Wingham and others (1998) reported a 11.7 ± 1.0 cm a^{-1} thinning trend averaged over the Pine Island Glacier and Thwaites Glacier drainage basins for the period 1992-1996, also from ERS data. While research on ice stream discharge from West Antarctic ice sheet has advanced, less attention has been given to the state of balance of the inland ice.

In this paper, surface elevation changes (dH/dt) are derived from ERS-1 and ERS-2 radar altimeter data for the period April 1992 through April 1999 and mapped on a 50-km grid for the region of West Antarctica south to 81.5° S between 10° W and 170° W. Elevation time-series, H(t), are constructed for selected areas from sets of elevation differences measured by the satellite radar altimetry at orbital-crossovers. A multivariate linear/sine function is fitted to the H(t) series to obtain linear trends of dH/dt and account for seasonal variations in the elevation measurement. Surface elevation changes are equivalent to ice thickness changes plus the vertical motion of the bedrock, which is generally smaller and can be separately estimated (Huybrechts and LeMeur, 1999). In addition, short-term changes caused by variations in rates of near-surface firn compaction must be considered (Arthern and Wingham, 1998; Wingham, 2000; and Zwally and Jun, submitted).

2. METHODS AND BACKGROUND

The ERS altimeters operated in either the ocean mode with a resolution of 45 cm per range gate or ice mode with a resolution of 182 cm per range gate. We use only ice mode data in this analysis because of a spatially variant bias between the modes and the greater spatial and temporal coverage of the ice mode data. We applied our V4 range-retracking algorithm, atmospheric range corrections, instrument corrections, and an adjustment for solid tides (Zwally and Brenner, 2001). We use the DUT DGM-E04 orbits that have a radial orbit precision of 5 to 6 cm (Sharroo and Visser, 1998). Based on analysis of global sea level changes with ERS-1and 2 data, TOPEX/Poseidon data, and tide gages, the long-term error in the ERS measurements over oceans due to unresolved instrumental trends and/or trends in orbital-errors appears to be < 1 cm a^{-1} (B. Beckley, Pers. Comm.)

Elevation changes are derived from surface elevation differences, $dH_{21} = H_2 - H_1$, measured at crossover locations where sub-satellite paths intersect at successive times t_2 and t_1. Since the measurement error for each dH_{21} is usually larger than the actual elevation change, a set of N values of $(dH_{21})_i$ must be averaged over a selected area to reduce the error of the mean. The average height difference, D_{ij} , at crossovers between orbit tracks in time interval i and those in a later interval j is calculated by

$$D_{ij} \equiv dH_{ij} = [1/N_{ji} \sum (A_j (t_j) - C_i (t_i)) + 1/M_{ij} \sum (C_j (t_j) - A_i (t_i))]/2 \qquad (1)$$

where N_{ji} is the number of crossovers between ascending passes at time j and descending passes at time i, A_j and C_i are the respective measurements of surface elevations, $t_j > t_i$, and similarly for the second term. Averaging of the separate calculations of the A-C and C-A averages cancels ascending versus descending biases, and subtracting A-C and C-A terms instead of summing gives the Asc-Des bias, as used in Zwally and others (1989) and Wingham and others (1998). Asc-Des biases can be caused by biases in orbital calculations, along-track timing errors

interacting with the slope of the orbit relative to the surface slope, or differences in the directional measurement properties of the radar signal.

Elevation time series, H(t), are constructed from sequences of average crossover differences in selected areas (e.g. 200 km circles) of the ice sheet. The areas of the ice-sheet selected for construction of the time-sequence must be sufficiently large (e.g. 200 km circles) to include an adequate number of crossovers to reduce the variances of the mean D_{ij}. The H(t) sequences are then fit with a multivariate linear and seasonal sinusoid to obtain an dH/dt trend and a seasonal variation. The period of the sinusoid is fixed at one year and the amplitude, phase, linear slope, and intercept are fitted parameters. Crossover differences between the first time interval t_1 (e.g. the first 90 days) and all successive intervals form a sequence of surface elevations versus time,

$$DS_{1N}(t) = D_{11}(t_1), D_{12}(t_2), D_{13}(t_3), D_{14}(t_4), \ldots\ldots D_{1N}(t_N) \qquad (2)$$

where $D_{11} = 0$ is the reference level. Additional sequences are created by crossovers between the second time interval, t_2, and successive intervals, and so forth for sequences starting with t_3, $\ldots\ldots t_{N-1}$. The D sequences are then combined into one elevation sequence ,

$$H(t) = H_1(t_1), H_2(t_2), H_3(t_3), \ldots\ldots H_N(t_N) \qquad (3)$$

where

$$H_1(t_1) = D_{11} = 0\ ,\ H_2(t_2) = D_{12},\ H_3(t_3) = 1/2\ [(D_{13} + (H_2 + D_{23})],$$
$$H_4(t_4) = 1/3\ [(D_{14} + (H_2 + D_{24}) + (H_3 + D_{34})], \ldots\ldots\ldots\ldots$$
$$H_N(t_N) = 1/(N-1)\ [D_{1N} + (H_2 + D_{2N}) + \ldots\ldots + (H_{N-1} + D_{N-1,N})]$$

The reference level $D_{22}(t_2) = 0$ of the second sequence is tied to the second point $H_2 = D_{12}$ of the first sequence. The third point H_3 then becomes the average of the change D_{13} from 1 to 3 and a second value, which is the change H_2 from 1 to 2 plus the change D_{23} from 2 to 3 from the second sequence, and so forth for all H_N. Variances of the mean are also calculated for each D_{ij} and

used to inversely weight the averages in calculating the H_N for the combined sequence. We also require that both N_{ji} and $M_{ji} \geq 5$ after performing a convergent 3-σ edit in calculating the A-C and C-A averages in D_{ij} .

As the length of the time sequence increases, the number of data crossovers increases in proportion to time squared. For an average of M crossovers between pairs of N time intervals, the total number of crossovers in the first time sequence would be N x M. However, the total number of crossovers in the combined H(t) sequence is $M \times \sum_1^N (n) = M \times N(N+1)/2$, which is (N+1)/2 times larger. Wingham and others 1998 used the first time sequence consisting of 33 successive 35-day repeat-orbit periods of ice mode data between 1992 and 1996, but the complete sequence has about 17X as many crossovers. If longer time intervals are used to construct the sequence, e.g. 70 days instead of 35, then 2X as many crossovers are used in the first sequence, and the total sequence would have 8.5X as many as the first sequence.

A detailed investigation of possible correlations between variations of radar backscatter power and altimeter-derived elevation changes in Greenland found no significant correlations in either seasonal or long-term variations (Brenner and others, 2000). Davis and others (2001) also found no significant correlation between elevation changes and backscattered power changes in East Antarctica, and therefore no need for a backscattering correction as was applied by Wingham and others (1998) for Antarctica. For the Pine Island glacier area of West Antarctica, Shepherd and others (2001) also applied no backscattering correction.

For West Antarctica, we mapped the altimeter measured power (P) for each 90-day period. We define P as the amplitude of the first peak of our retracked waveform fit, normalized by the instrument AGC (Automatic Gain Control). During the overlap period, our measured ratio of the average P for ERS-1 to that for ERS-2 over all of Antarctica is 2.06. Therefore, we multiplied the ERS-2 measured powers by 2.06 before analyzing trends in P. Our linear-sinusoidal multivariate fit to the time series of P at each grid point gives the dP/dt trend, the p-p seasonal amplitude, and the phase of the seasonal variation of P. For the area of West Antarctica

mapped in the next section, the resulting linear correlation coefficients (R) are low: R= 0.10 between dH/dt and dP/dt, R= 0.26 between the amplitudes of P(t) and H(t), and R=0.33 between the phases. Although significant correlations between dH/dt and dP/dt may be found in some regions, the correlations are negative in some regions, positive in others, and show a wide scatter of points in all quadrants with a low overall correlation (Figure 1). Therefore, we make no backscattering correction to dH/dt. The mean and standard deviation of the dH/dt are 0.22 cm a^{-1} and 19.0 cm a^{-1} and of the power change, dX/dt, are 0.01 and 0.023 a^{-1} (using $X= \log_{10}(P/10^5)$). These correlation results, however, are specific to our particular range-retracking algorithm, which selects the mid-point of the leading waveform ramp, and might not apply to other algorithms that have different sensitivities to peak power variations, to variations in the integrated power in the waveform, or the ratio of surface to subsurface volume scattering.

Analysis of crossovers between ERS-1 and ERS-2 during the 12 months of simultaneous operation from April 1995 to April 1996 allowed determination of a significant spatial-variant bias between ERS-1 and ERS-2 ice mode data. In Greenland the bias of ERS-2 minus ERS-1 elevations varied between about 3 cm at higher elevations to about 25 cm at lower elevations. The magnitude of the bias was found to be well correlated with each of three parameters, the measured backscatter power, surface slope, and surface elevation, all of which are interrelated. Backscatter power is strongly correlated with surface slope because of the angle-dependent effects of beam attenuation on the radar signal. On ice sheets, surface slope and surface elevation are generally inversely correlated. In West Antarctic, we characterize the bias as a linear function of elevation (bias (cm) = -0.004272 X(m) + 19.53, where X is elevation), which is based on crossover bias measurements of 16.3 cm for 700 to 1200 m, 12.05 cm for 1200 to 1700 m, 11.05 cm for 1700 to 2200 m, and 9.53 cm for 2200 to 2700 m elevation. For elevations with the grid center elevation $\leq$ 150 m, which are mostly low-slope locations on ice shelves and glacier tongues, the ERS1-2 bias correction is fixed at 9 cm, which is an estimate of the asymptotic value for low slopes. Using this fixed bias for low-elevation/low slope areas, instead of the linear function of elevation, adjusts the dH/dt values by about + 2 cm a^{-1}.

A recent analysis and modeling of the H(t) time series for the GISP2 "summit" of Greenland (72° 34' N, 38° 27' W, 3200 m) for 1992 to 1999 showed agreement between the modeled and observed seasonal cycles (in both amplitude and phase) and significant interannual variations during 1992 to 1999 (Zwally and Jun, submitted). In addition, the derived dH/dt = + 4.2 2.9 cm a^{-1} from the altimeter H(t) series agrees well with the +3.6 ± 2.1 cm a^{-1} obtained by Hamilton and Whillans (2000) using the GPS coffee-can method. The altimeter dH/dt analysis included crossovers within a 200 km diameter circle and ± 250 m elevation of the summit. The observed amplitude of the seasonal elevation cycle was 25 cm peak-to-peak (p-p) with a minimum in July. This amplitude is larger than expected on the basis of seasonal variations in precipitation, which are small in the summit region. Similar seasonal variations that were previously reported in other satellite altimetry data were unexplained by either by variations in the effective depth of the radar measurement or other measurement characteristics (Yi and others, 1997). However, the elevation model by Zwally and Jun (submitted) uses a stronger temperature-dependent rate of firn compaction than previous models and shows that most of the annual compaction of the upper layers of firn occurs during the warmer spring and early summer months, giving an elevation minimum in mid-summer. We find a similar seasonal cycle of surface elevation in parts of West Antarctica, but the emphasis here is on analysis of the dH/dt trends.

3. RESULTS AND DISCUSSION

For the region of West Antarctica from 10° W to 170° W (Figure 2), we construct H(t) sequences and derive a dH/dt value using linear-sinusoidal multivariate fit for each 50-km grid point (Figure 3). Crossovers lying within a 200 km circle and ± 250 m elevation of the grid center are selected for the H(t) sequences constructed using time periods of t_i = 90 days. For slopes > 1/800 using the 200 km circle, the elevation limitation restricts the selected areas to bands along elevation contours, where the elevation changes tend to be spatially coherent. For specific locations noted in Figure 2, a smaller (100 km) circle is used for crossover selection to construct the H(t) series shown in Figures 4 - 7. For the specific low-elevation locations on ice shelves, a

smaller elevation limitation of -30 m to + 100 m is also used to eliminate crossovers over ocean or sea ice areas. Over ice shelves, no correction is made for the vertical motion of the ice shelves that is forced by ocean tides, which increases somewhat the random errors in the H(t) sequence and the derived dH/dt.

Ice Shelves and Ice Stream E

On the major Ross and Filchner-Ronne ice shelves, the dH/dt trends in Figure 3 are mostly within one standard deviation of zero. At a particular location (80.5° S, 155° W, 90 m) on the Ross Ice Shelf, the dH/dt is +0.2 ± 1.8 cm a^{-1} as shown in Figure 4. On the Filchner Ice Shelf at (79.03° S, 39.81° W, 95 m), the dH/dt is + 2.7 ± 2.3 cm a^{-1}. Also, on the lower part of Ice Stream E (79.7° S, 140° W, 460 m), in an area close to where Bindschadler and others (1996) calculated a thickness change of + 22 ± 103 cm a^{-1} from differences in measured fluxes through ice-stream gates, the altimeter-derived dH/dt is +1.4 ± 1.9 cm a^{-1}.

The finding of near-zero dH/dt values on the Ross and Filchner-Ronne Ice shelves provides a geophysical reference against which the accuracy of larger positive and negative dH/dt values obtained for other areas can assessed. Although expected changes in ice-shelf thicknesses might be comparable to those on the grounded ice-sheets, changes in ice-shelf surface elevation for a particular change in thickness would be only about 1/6 as large because the shelves are floating. In addition, the large contrast in dP/dt backscatter trends between the two ice shelves provides information on the validity of not making a backscattering correction, as discussed in the last section. The larger trend of dP/dt = 0.060 on the Ross Ice shelf compared to a near-zero trend of 0.001/yr on the Filchner, indicates that any significant adjustment for a relation between dH/dt and dP/dt would make the dH/dt on the Ross shelf significantly negative.

The seasonal variation for the first 2 or 3 cycles in the Ross Ice Shelf (Figure 4), in particular, are not as well defined as later in the series. The H(t) series improve in accuracy with time, partly because of more early gaps when the altimeters was in ocean mode, and partly because of a

characteristic of the construction of the H(t) series. Generally, the H(t) accuracies improve with time because more and more terms of the Eq. 2 sequences are averaged with increasing time in the combined sequence of Eq. 3. Alternatively, the H(t) can be constructed backwards with improving accuracy toward earlier times. For the Ross Ice Shelf location, the seasonal cycle is well defined with a 53 ± 7 cm peak-to-peak amplitude. The occurrence of the minimum in April 27 just after the warm season is consistent with the firn compaction model of Zwally and Li (submitted). In contrast, the 20 ± 9 cm amplitude on the Filchner Ice Shelf and the 17 ± 8 cm amplitude on Ice Stream E are less well defined and might not represent a clear seasonal cycle.

The ice shelves along the Antarctic Peninsula and the coast of West Antarctica all show significant decreases in surface elevation, in marked contrast to the Ross and Filchner-Ronne Ice shelves. These more northerly ice shelves are in a warmer climatic regime, which also has been warming in recent decades. Recent breakups of the ice shelves in the Antarctic peninsula have been shown to be associated with the regional climatic warming (Doake and Vaughan, 1991; Skvarca and others, 1998; Scambos and others, 2000). On the Larsen Ice Shelves, the derived thinning rates range from about 25 cm a^{-1} on Larsen "B" area around 65.5° S, to 22.7 ± 2.3 cm a^{-1} at (67° S, 62.5° W, 43 m) (Figure 5), to about 5 cm a^{-1} at the southernmost part around 69° S. Using an average value of 0.16 for the ratio of the height of the freeboard to ice shelf thickness (Thomas, 1973), implies an ice shelf thickness change of 142 ± 14 cm a^{-1} at (67° S, 62.5° W, 43 m), which is about 0.5% of the thickness per year. This calculation implicitly assumes no change in the firn density profile. If the elevation change represents a decrease in firn thickness rather than an assumed decrease in the thickness of solid ice, the implied decrease in ice shelf thickness would be smaller.

The largest thinning rates (Figure 3) are located along the coast from the outlets of the Pine Island Glacier at 100° W and the Thwaites Glacier at 107° W to the vicinity of the Dotson Ice Shelf at 112° W. The coast from 110 W to 135 W includes the Dotson Ice Shelf, the Getz Ice Shelf, and a number of ice-covered promontories. Therefore, for these locations crossovers lying both on ice shelves and on grounded ice can be included within the 200 km cap size and the ±

250 m limits used in making the dH/dt map. However, the H(t) for the Dotson Ice shelf location (74.91° S, 111.80° W) in Figure 5 is restricted to crossovers within + 100 m and -30 m of the 83 m elevation at the center of the cap. Therefore, the 64.9 ± 4.2 cm a^{-1} elevation decrease is mostly indicative of ice shelf thinning that could be as large as 4 m a^{-1} decrease in thickness.

Regional averages of the grid points in the dH/dt map with central elevations in the range of 30 to 150 m represent mostly average changes in ice shelf elevations (Table 1). Although the overall averages for the Ronne- Eastern Filchner and the Ross ice shelves are close to zero (< +1 cm a^{-1}) spatial variations at the + 5 to - 5 cm a^{-1} could be significant. In particular, most dH/dt on the Filchner ice shelf are positive, whereas those on the Ronne ice shelf (circa 160° W) are negative. Also, the values for the portion of the Ross Ice shelf east of Roosevelt Island (circa 160° W) are positive, whereas the values to the southeast are negative. The average elevation change on the Riiser-Larsen and Brunt ice shelves (10° W - 30° W) is an increase of 2.42 cm a^{-1}. The average dH/dt on the Western Ronne ice shelf is - 2.86 cm a^{-1}, and the averages for the ice shelves of the Antarctic Peninsula and along the West Antarctic coast are significantly negative from about 7 to 17 cm a^{-1}.

Pine Island Glacier and Thwaites Glacier Drainage Basins

The sets of H(t) for the Pine Island Glacier and Thwaites Glacier drainage basins in Figures 6 and 7 extend inland from the glacier tongue and across the respective ice divides (Figure 2). For the Pine Island Glacier line, the thinning extends to the ice divide and the dH/dt becomes positive by 3.8 ± 2.1 cm a^{-1} on the other side of the divide. For the Thwaites Glacier, the dH/dt becomes positive just before the divide and is positive > 10 cm a^{-1} on the other side. The maximum elevation decrease on the Pine Island glacier is 61 ± 11 cm a^{-1} at the outlet (75.2° S, 99° W), which is not as large as the 360 ± 90 cm a^{-1} obtained by at (75.3° S, 99° W). The technique used by Shepherd and others (2001) analyzes changes at specific repeat-track crossover points and resolves the 30 km wide glacier better than our 100 km cap size does. Inland to about 95 W, the larger rates of elevation decrease are mostly confined to the glacier trunk (Figure 3), as noted by

Shepherd and others, 2001. However, significant increases (≈5 to 20 cm a^{-1}) occur over most of both the Pine Island Glacier and the Thwaites Glacier drainage basins (outlined in Figure 2).

Marie Byrd Land

Significant elevation increases (≈ 10 cm a^{-1}) are observed along the ice-divide between the Thwaites drainage basin and the drainage basin for Ice streams D, E, and F flowing into the Ross Ice Shelf (Figure 3). The H(t) series centered at (80 S, 120 W,526 m) shows a dH/dt increase of 9.0 ± 1.6 cm a^{-1} and a peak-to-peak seasonal amplitude of 67 cm with a minimum in March 5. For comparison, a recent coffee-can/GPS measurement at Byrd station gave an elevation-change close to zero (-0.4 ± 2.2 cm a^{-1}) (Hamilton and others, 1998). Steig and others (2001), using the elevation-dependence of stable isotopes obtained from ice cores, calculated an elevation rise at Byrd station of about 150 m during the last 2 Ka (≈ +7 cm a^{-1}), which would be consistent with our observation if this average rate were continuing.

The rate of present-day bedrock uplift, calculated from the holocene ice unloading in West Antarctica, is about 3 to 7 cm a^{-1} (Huybrechts and Le Meur, 1999). Therefore, the rate of ice thickening implied by the surface dH/dt of +9 cm a^{-1} would be in the range of +2 to +6 cm a^{-1}. In contrast, ice flow and continuity studies near Byrd Station indicated a small ice thinning of 3 cm a^{-1} (Whillans,1977).

To the south of Byrd Station, the dH/dt is larger, in the range of +15 to +20 cm a^{-1}. Along the ice divide to the north of Byrd, the dH/dt is rather uniformly positive at about 8 to 10 cm a^{-1}. At the point (76 S, 127 W, 2225 m) in the Executive Committee Range the elevation increase is 22.2 ± 3.0 cm a^{-1} (Figure 8), and is similarly significantly positive along this east-west ridge near the northernmost part of the ice sheet. For comparison, the elevation change map shown by Wingham and others (1998) from ERS data for 1992 to 1996 also appears to be mostly positive extending along the ice divide from near Byrd to the north and then northwest, but is not clearly positive or negative in the vicinity of Byrd station.

Average Elevation Changes and Mass Balance Implications

Average elevation changes are calculated for 500 m elevation bands and for longitudinal sectors (Table 2). Grid points with central elevations < 150 m are excluded in order to restrict the analysis to mainly grounded ice. The corresponding rates of ice mass loss and sea level rise, making no correction for motion of the bedrock, are also given in Table 2. The overall net change in elevation is 1.2 cm a^{-1}, which would correspond to a mass gain of 20 Gt a^{-1}, and a -0.06 mm a^{-1} change in global sea level. The density of solid ice is used to convert from elevation change to mass change, which is equivalent to assuming the changes are long-term and not a result of very recent changes in the accumulation of lower density firn. Calculations of the bedrock motion (Huybrechts and Le Meur, 1999) range from about 0.2 to 1 cm a^{-1} in the Antarctic Peninsula, to about 1 to 2 cm a^{-1} along the West Antarctic Coast, to about 7 to 10 cm a^{-1} in the central portion of the grounded ice sheet. However, the magnitude of the uplift over central West Antarctica (up to 10 cm/year) may be at the high side because of a late deglaciation produced by the ice-evolution model (Huybrechts, Pers. Com.) Using an average uplift of 2.5 cm a^{-1} implies an average ice thickness decrease of 1.3 cm a^{-1}, a mass loss of 22 Gt a^{-1}, and a 0.06 mm a^{-1} contribution to global sea level rise. (Not by authors: uplift averages will be calculated better from Huybrechts data for final version of paper.)

Although the overall average elevation or thickness changes suggest the grounded ice is close to balance, the average elevation for the Pine Island-Thwaites basin sector is significantly decreasing by 8.1 cm a^{-1}. The corresponding ice thickness change is about -11 cm a^{-1}, with a corresponding mass loss of 82 Gt a^{-1}, and a 0.22 mm a^{-1} contribution to global sea level rise. In terms of elevation change, the decrease in the Pine Island-Thwaites sector sector is largely balanced by the increase in the Marie Byrd Land, but only balanced by about 1/4 in terms of ice thickness change and contribution to sea level rise.

4. CONCLUSIONS

Present-day changes in ice sheet surface elevation are a combination of long-term ice dynamics and recent changes in the surface balance. One representation of the present-day dynamic evolution of the ice thickness and surface elevation, from a coupled 3-D ice dynamic model and solid-Earth model (Huybrechts and Le Meur, 1999), shows an increase in elevation of grounded ice in Coates Land, the Antarctic Peninsula, and a narrow coastal band of the West Antarctic ice sheet between about 130° W and 145° W. Our dH/dt results are also positive in these regions. Over most of the rest of the West Antarctic ice sheet including the Pine Island-Thwaites drainage basin, the coupled model shows thinning. Although the decreases in the model are only about 1/10 as large as our dH/dt, the qualitative agreement suggests that the long-term ice dynamic changes captured in the model are also observed in the data. For the Pine Island Glacier, Shepherd and others (2001) said the thinning cannot be explained by short-term variability in accumulation and must result from glacier dynamics. Similarly over the Thwaites Glacier drainage basin, a reduction of accumulation (Giovinetto and Zwally, 2000) by about 50% would be required to produce the observed elevation decrease. In contrast to these regions of qualitative agreement, the observed surface elevation increases over Marie Byrd Land and south of the ice divide in the Pine Island-Thwaites basin sector are opposite in sign to the elevation decreases in the model. If the uplift in this region were smaller than the model (see note in previous section), the discrepancy would be even larger. Therefore, an accumulation increase of the order of 30 to 50% would be required to explain the observed increase in elevation in these areas.

Expected consequences of climate warming in polar regions are an increase in precipitation and an increase in summer melting. Present-day surface melting in Antarctic is mostly confined to the ice shelves (Zwally and Fiegles, 1994), and is therefore not a factor in the observed elevation changes. However, the increase in surface elevation in Marie Bryd Land would be consistent with an increase in precipitation in recent decades. As noted in previous sections, recent breakup of ice shelves in the Antarctic Peninsula have been associated with climatic warming. The observed dH/dt decreases on the ice shelves in the Peninsula and along the West Antarctic

coast are a direct indication of significant thinning of the shelves remaining in those regions, perhaps due to both surface and bottom melting. In contrast, the major Ross, Filchner, and Ronne ice shelves lie in colder climatic regimes were surface melting is infrequent (Zwally and Fiegles, 1994), and the observed dH/dt are close to zero. The small values of dH/dt on the major ice shelves also provides a reference for assessing the validity of the larger observed dH/dt values elsewhere. Nevertheless, there are some notable variations in dH/dt over these shelves that may prove to be significant with further analysis.

Table 1. Regional elevation changes for grid points with central elevations between 30 m and 150 m, which are primarily ice shelves. N is number of 50 km grid cells.

Elevation Band 30- 150 m	Risser-Larsen & Brunt 10W - 30W		Filchner - E. Ronne 30W - 60W		W. Ronne 76S - 82S 60W - 85W		Peninsula Shelves 64 S-76 S 60 W-85 W		Pine Island - Thwaites, Dotson 85W - 115W		Getz 115W - 150W		Eastern Ross Ice Shelf 150W - 170W	
	N	dH/dt*	N	dH/dt*	N	dH/dt*	N	dH/dt*	N	dH/dt*	N	dH/dt*	N	dH/dt*
Area (10^5 km^2)	8	0.45	72	1.80	71	1.78	47	1.18	22	0.55	22	0.55	37	0.93
dH/dt (cm a^{-1})		2.42		0.85		-2.86		-7.42		-17.03		-8.78		0.70

Table 2. Regional average elevation changes dH/dt (cm a^{-1}), dMass/dt (Gt a^{-1}), and sea-level equivalent rate (mm a^{-1}). *Values are dH/dt (cm a^{-1}) unless noted in left column. N is number of 50 km grid cells. Without correction for bedrock motion, the overall net change is 1.2 cm a^{-1}, 20 Gt a^{-1}, and -0.06 mm a^{-1} sea level equivalent.

	Coates Land 10W - 30W		Berkner Island 30W - 60W		South of Ant. Pen. 76S - 82S 60W - 85W		Antarctic Peninsula 64 S-76 S 60 W-85 W		Pine Island - Thwaites Basin 85W - 115W		Marie Byrd Land 115W - 150W		Roosevelt Island + 150W - 170W	
Elevation Band	N	dH/dt*	N	dH/dt*	N	dH/dt*	N	dH/dt*	N	dH/dt*	N	dH/dt*	N	dH/dt*
2200-2700 m	2	3.66							4	3.13	5	13.46		
1700-2200 m	30	5.38					15	20.14	65	5.59	48	9.00		
1200-1700 m	43	3.97			2	-5.42	26	11.14	69	-6.37	62	9.28		
700-1200 m	38	2.64	12	-2.93	14	0.46	39	4.38	63	-12.44	45	6.75	4	6.38
150-700 m	20	2.48	17	0.08	37	-0.48	23	4.61	15	-60.52	39	-1.13	11	-0.64
Wt'd Avg.		3.68		-1.17		-0.42		8.43		-8.13		6.71		1.37
Area (10^5 km^2)		3.33		0.73		1.33		2.58		5.40		4.98		0.35
dMass/dt (Gt a^{-1})		11.2		-0.8		-0.5		19.9		-40.2		30.6		0.4
Sea level (mm a^{-1})		-0.03		0.00		0.00		-0.06		0.11		-0.08		0.00

REFERENCES

Alley, R. B. and R. A. Bindschader. 2001. The West Antarctic Ice Sheet and sea level change. in *The West Antarctic Ice Sheet: Behavior and Environment,* AGU Antarctic Research Series **77,** 1-11.

Arthern, R.T. and D. J. Wingham. 1998, The natural fluctuations of firn densification and their effect on the geodetic determination of ice sheet mass balance, *Climate Change,* **40**, 605-624.

Brenner, A.C., H. J. Zwally, H. Cornejo, and J. L. Saba, 2000. Investigation of correlations between variations of radar backscatter with altimeter-derived ice sheet elevation changes and ERS-2/ERS-1 biases, *Proc. ESA ERS-Envisat Symposium, ESA.*

Bentley, C. R., 1997, Rapid sea-level rise soon from West Antarctic ice sheet collapse?, *Science* **275**, 1077.

Bindschadler, R. 1998. Future of the West Antarctic Ice Sheet, *Science* **282**, 428-429.

Bindschadler, R., P. Vornberger, D. Blankenship, T. Scambos, and R. Jacobel. 1996. Surface velocity and mass balance of Ice Streams D and E, West Antarctica, *J. Glaciol.*, 42 (142) 461-475.

Davis, C.H., R.G. Belu, and G. Feng. 2001. Elevation change measurement of the East Antarctic ice sheet, 1978-1988, from satellite radar altimetry, *IEEE Transactions on Geoscience & Remote Sensing*, **39**, (3) 635-644.

Doake, C. S. M. and D. G.Vaughan. 1991. Rapid disintegration of the Wordie Ice Shelf in response to atsmopheric warming. Nature, 350 (6316), 328-330.

Hamilton, G. S., I. M. Whillans, P. J. Morgan. 1998. First point measurements of ice-sheet thickness change in Antarctica, *Ann. Glaciol.* **27,** 125-129.

Hamilton, G. S. and I. M. Whillans, 2000. Point measurements of mass balance of the greenland ice sheet using precision vertical global positioning system (GPS) surveys, *J. Geophys. Res.,* **105**, B7, 16,295-16,301.

Huybrechts, P. and E. Le Meur, 1999. Predicted present-day evolution pattern of ice thickness and bedrock elevation over Greenland and Antarctica, *Polar Record*, **18** (2) 299-306.

Oppenheimer M. 1998. Global Warming and the Stability of the West Antarctic Ice Sheet, *Nature* **393,** 325-332.

Rignot, E.1998. Fast recession of a West Antarctic glacier, *Science*, **281**, 549-551.

Scambos, T. A., C. Hulbe, M. Fahnestock, and J. Bohlander. 2000. The link between climate warming and break-up of ice shelves in the Antarctic Peninsula. *J. Glaciol.*, **46** (154) 516-530.

Sharroo, R. and P. Visser, 1998. Precise orbit determination and gravity field improvement for the ERS Satellites", *J. Geophys. Res.*, **103**, (C4), 8113-8127.

Shephard, A., D. J. Wingham, J. A. C. Mansley, and H. F. J. Corr, 2001. Inland thinning of Pine Island Glacier, West Antarctica. *Science*, **291**, 862-864.

Skvarca, P., W. Rack, H. Rott, and T. I. y Donangelo. 1998. Evidence of recent climatic warming on the eastern Antarctica Peninsula, *Ann. Glaciol.* **27**, 628-632.

Steig, E. J., J. L. Fastook, C. Zweck, I. D. Godwin, K. J. Licht, J. W. C. White, and R. P. Ackert Jr. 2001. West Antarctic elevation changes, in *The West Antarctic Ice Sheet: Behavior and Environment,* AGU Antarctic Research Series **77,** 75-90.

Thomas, R. H., The creep of ice shelves: interpretation of observed behaviour. *J. Glaciol.*, **19** (64) 55-70.

Vaughan, D. G., A. M. Smith, H. F. J. Corr, A. Jenkins, C. R. Bentley, M. D. Stenoien, S. Jacobs, T. B. Kellogg, E. Rignot, and B. Lucchitta, 2001. A review of Pine Island Glacier, West Antarctica: hypotheses of instability vs. observations of change, in *The West Antarctic Ice Sheet: Behavior and Environment,* AGU Antarctic Research Series **77,** 237-256.

Whillans, I. 1977. The equation of continuity and its application to the ice sheet near Byrd station Antarctica, *J. Glaciol.,* **18** (80) 359-372.

Wingham, D.J., Ridout A.J., Scharroo R., Arthern R.J., Shum C.K. 1998. Antarctic elevation change from 1992 to 1996, *Science,* **282**, 456-458.

Wingham, D.J. 2000. Small fluctuations in the density and thickness of a dry firn column. *J. of Glaciol.*, **46,** 154, 399-411.

Yi, D., C. R. Bentley and M. D. Stenoien. 1997. Seasonal variation in the apparent height of the East Antarctic ice sheet. *Ann. of Glaciol.*, **24**, 191-198.

Zwally, H. J., A. C. Brenner, J. A. Major, R. A. Bindschadler, and J. G. Marsh. 1989. Growth of the Greenland ice sheet: measurement. Science **246**,1587-1589

Zwally, H. J. and A. C. Brenner, 2001: Ice sheet dynamics and mass balance, Chap. 9 in *Satellite Altimetry and Earth Sciences,* ed by Lee-Lueng Fu and Anny Cazenave, Academic Press, 351-

369.

Zwally, H. J. and S. L. Fiegles. 1994. Extent and duration of Antarctic surface melting. *J. of Glaciol.*, **40** (136) 463-476.

Zwally H.J. and Jun L., (submitted) Seasonal and interannual variations of ice sheet surface elevation at the summit of Greenland, *J. Glaciol.*

LIST OF FIGURES

Figure 1. Scatter plot between 7-year elevation trends (dH/dt) and backscatter power trends (dX/dt, where $X = \log_{10}(P/10^5)$). Lack of correlation is shown by low $R = 0.10$. Mean and standard deviations indicated by solid and dashed lines, with values in text.

Figure 2. West Antarctic location map showing drainage basins and locations for the H(t) elevations series given in Figures 4 -8.

Figure 3. Elevation-change map of West Antarctic showing small or near-zero elevation changes on the Ronne, Filchner, and Ross Ice Shelves, and significant thinning on the ice shelves of the Antarctic Peninsula and along the West Antarctic coast. Over most of the drainage basins of Pine Island and Thwaites glaciers, the surface elevation is significantly decreasing. The elevation is increasing over most of the other grounded ice, including most of Marie Byrd Land, the Antarctic Peninsula, and Coates Land part of the East Antarctic ice sheet. The cap size for the H(t) crossover series for each 50-km grid cell is 200 km diameter and the elevation limit is ± 250 m of the elevation of the grid center. dH/dt values are from multivariate linear and seasonal sinusoidal fit to the H(t) series. Elevation-dependent ERS-1/ERS-2 bias correction is described in text.

Figure 4. H(t) time series created from crossovers among 90-day intervals for 3 locations (see Figure 2) on the Filchner ice shelf, Ross ice shelf, and ice stream E that flows into the Ross ice shelf. The dH/dt linear trend and the seasonal cycle are obtained from a multivariate linear and seasonal sinusoidal fit to the H(t) series. Cap size for crossover selection is 100 km diameter and the elevation limits are shown in Figure. dH/dt trends are near zero in these locations.

Figure 5. H(t) times series and dH/dt trends for 2 locations on the Larsen and Dotson ice shelves showing significant surface elevation decreases, with an implied shelf thinning six times larger. Analysis parameters are as in Figure 4.

Figure 6. H(t) times series and dH/dt trends for 6 locations on a line extending from the front of Pine Island Glacier drainage basin inland to the East and across the ice divide (see Figure 2). Significant elevation decreases occur up to the ice divide and a small elevation increase occurs on the other side of the divide. Analysis parameters are as in Figure 4.

Figure 7. H(t) times series and dH/dt trends for 7 locations on a line extending from the front of Pine Island Glacier drainage basin inland to the south and across the ice divide (see Figure 2). Significant elevation decreases occur until just before the ice divide and a significant elevation increases occurs on the other side of the divide. Analysis parameters are as in Figure 4.

Figure 8. H(t) times series and dH/dt trends for locations at Byrd Station, on the ice divide, and the Executive Committee Range on the ridge near the coast of West Antarctica. The elevation is significantly increasing in these locations. Analysis parameters are as in Figure 4.

Figure 1.

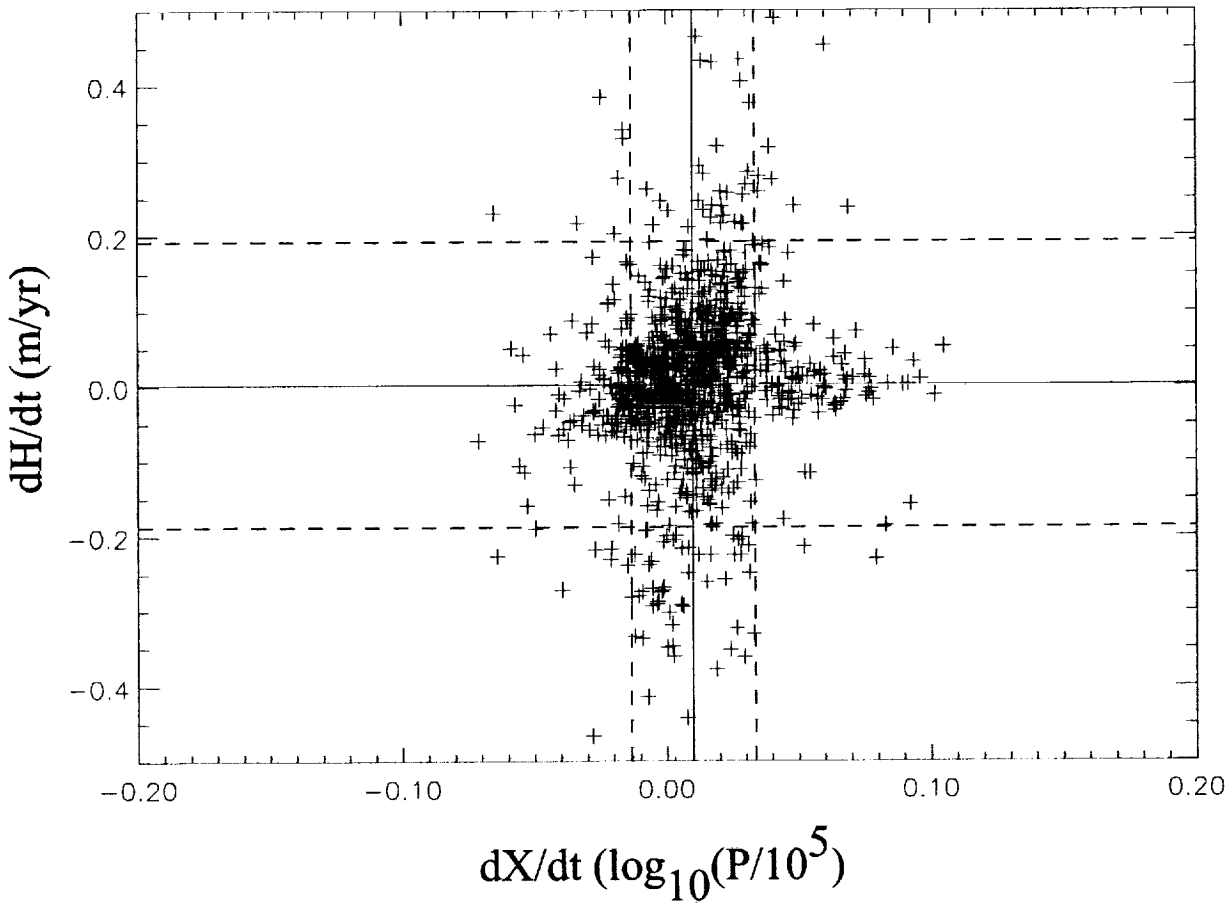

Figure 2.

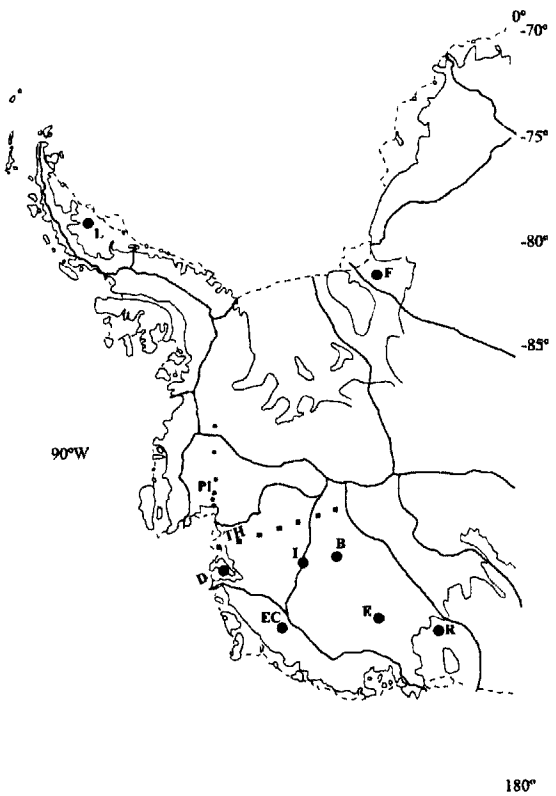

Figure 3.

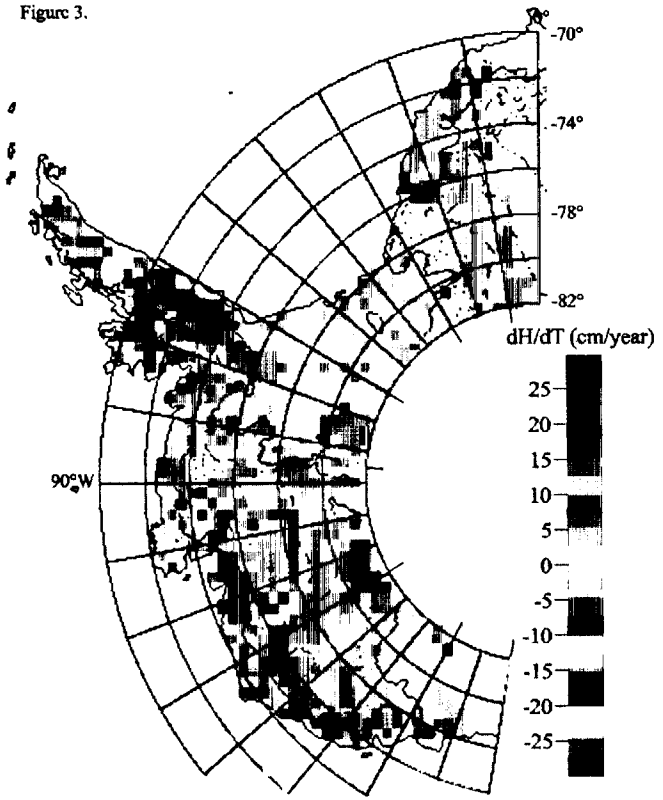

Fig. 4

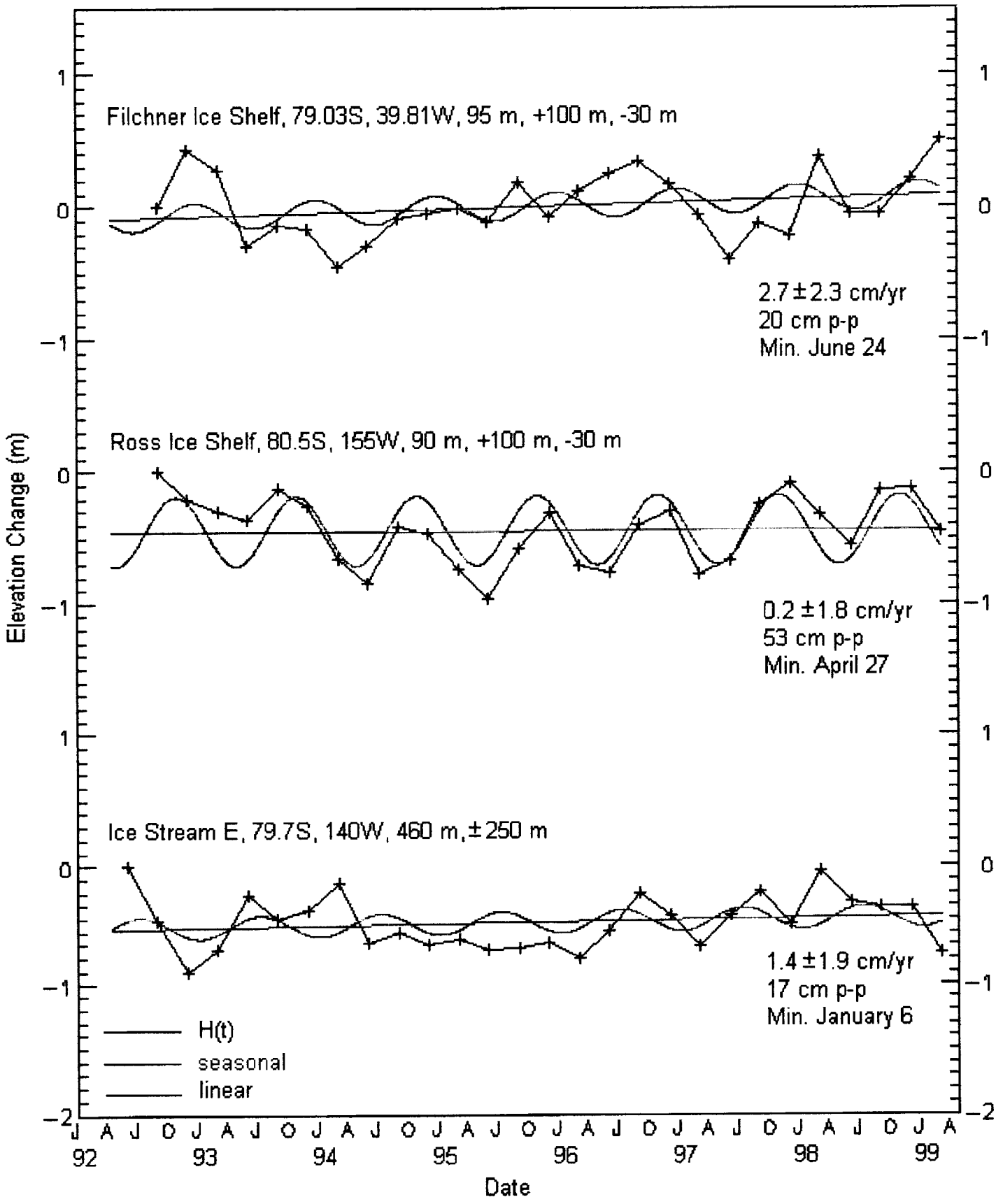
Filchner Ice Shelf, 79.03S, 39.81W, 95 m, +100 m, -30 m
2.7 ± 2.3 cm/yr
20 cm p-p
Min. June 24
Ross Ice Shelf, 80.5S, 155W, 90 m, +100 m, -30 m
0.2 ± 1.8 cm/yr
53 cm p-p
Min. April 27
Ice Stream E, 79.7S, 140W, 460 m, ± 250 m
1.4 ± 1.9 cm/yr
17 cm p-p
Min. January 6
H(t)
seasonal
linear
Elevation Change (m)
Date
J A J O J A J O J A J O J A J O J A J O J A J O J A J D J A
92 93 94 95 96 97 98 99

Fig. 5

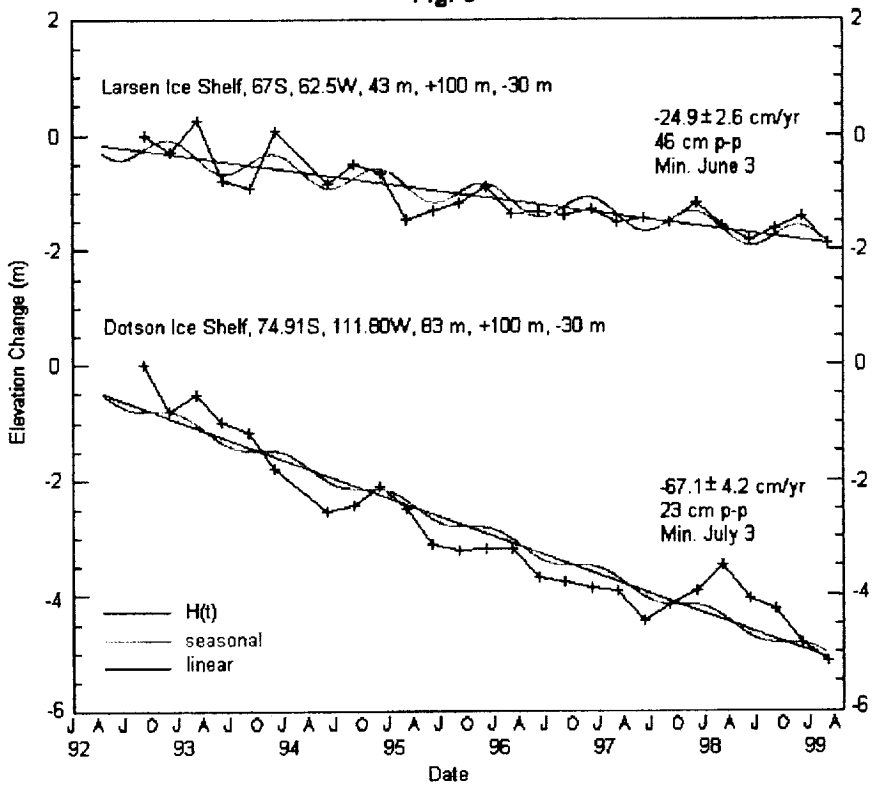
Larsen Ice Shelf, 67S, 62.5W, 43 m, +100 m, -30 m
-24.9 ± 2.6 cm/yr
46 cm p-p
Min. June 3
Dotson Ice Shelf, 74.91S, 111.80W, 83 m, +100 m, -30 m
-67.1 ± 4.2 cm/yr
23 cm p-p
Min. July 3
H(t)
seasonal
linear
Elevation Change (m)
2
0
-2
-4
-6
J A J O J A J O J A J O J A J O J A J O J A J O J A
92 93 94 95 96 97 98 99
Date

Fig. 8

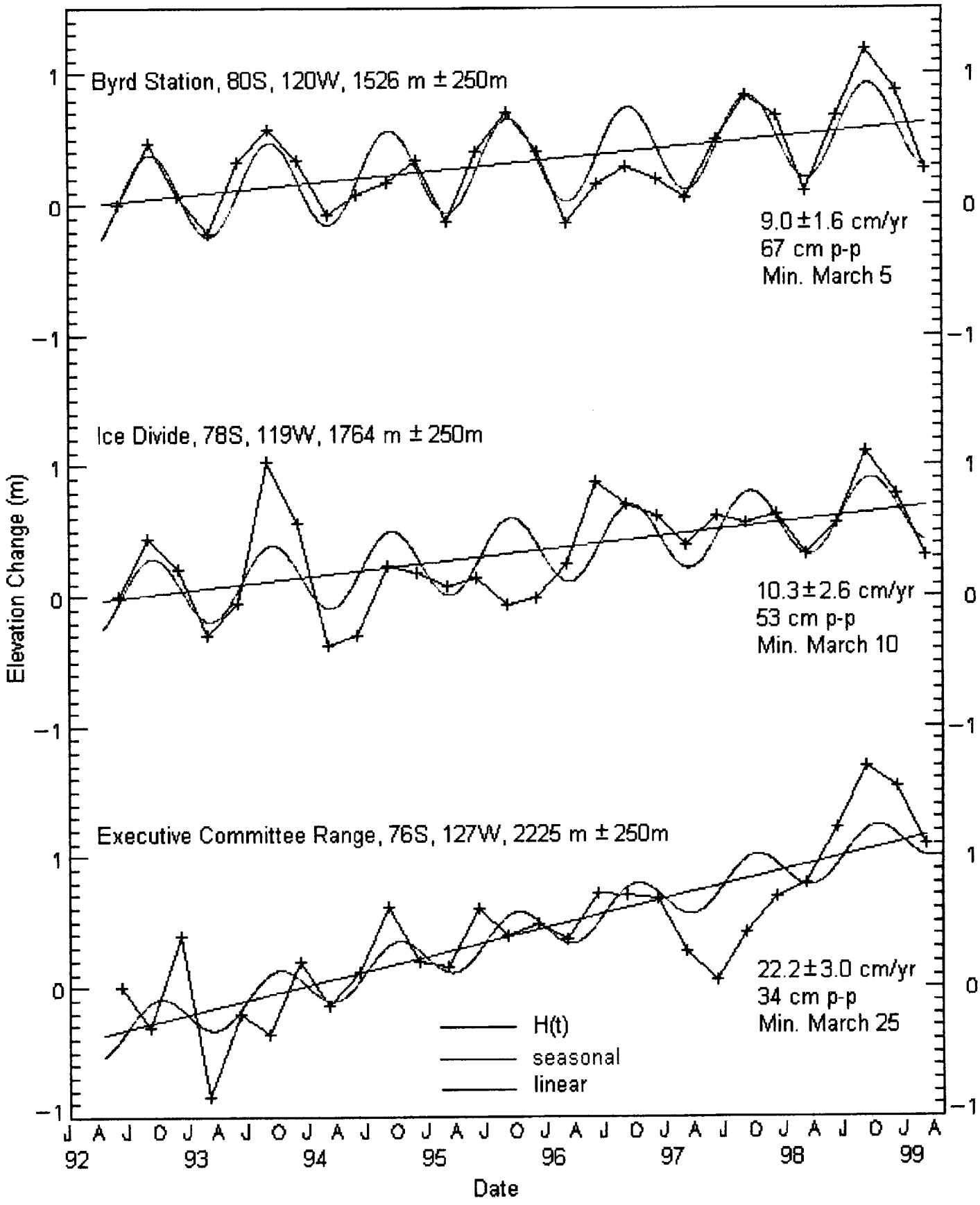
Byrd Station, 80S, 120W, 1526 m ± 250m
9.0 ± 1.6 cm/yr
67 cm p-p
Min. March 5
Ice Divide, 78S, 119W, 1764 m ± 250m
10.3 ± 2.6 cm/yr
53 cm p-p
Min. March 10
Executive Committee Range, 76S, 127W, 2225 m ± 250m
22.2 ± 3.0 cm/yr
34 cm p-p
Min. March 25
H(t)
seasonal
linear
Elevation Change (m)
1
0
−1
J A J O J A J O J A J O J A J O J A J O J A J O J A J O J A
92
93
94
95
96
97
98
99
Date

POPULAR SUMMARY
HJZ, August 22, 2001

Surface Elevation Changes in West Antarctica from Satellite Radar Altimetry: Mass Balance Implications

H. Jay Zwally, Anita C. Brenner, and Helen Cornejo

Antarctic ice-sheet surface elevation changes (dH/dt) are obtained from 7-years (1992-1999) of ERS-1 and 2 satellite radar altimeter data. On the major Ronne, Filchner, and Ronne ice shelves, the dH/dt are small or near zero. In contrast, the ice shelves of the Antarctic Peninsula and along the West Antarctic coast appear to be thinning significantly, with a 23 ± 3 cm/yr surface elevation decrease on the Larsen ice shelf and a 65 ± 4 cm/yr decrease on the Dotson ice shelf. Significant elevation decreases are obtained over most of the drainage basins of the Pine Island and Thwaites glaciers. Significant increases are obtained over most of the other grounded ice in Marie Byrd Land, the Antarctic Peninsula, and Coates Land. Over the sector from 85° W to 115° W, which includes the Pine Island and Thwaites basins, the average elevation is significantly decreasing by 8.1 cm/yr. The corresponding ice thickness change is about -11 cm/yr, with a corresponding mass loss of 82 Gt/yr, and a 0.22 mm/yr contribution to global sea level rise. In terms of elevation change, the decrease in the Pine Island-Thwaites sector sector is largely balanced by the increase in the Marie Byrd Land, but only balanced by about 1/4 in terms of ice thickness change and contribution to sea level rise. The overall average elevation change for the grounded ice is + 1.2 cm/yr. Using an average bedrock uplift of 2.5 cm/yr , implies an average ice thickness decrease of 1.3 cm/yr, a mass loss of 22 Gt/yr, and a 0.06 mm/yr contribution to global sea level rise.